Magazine of Civil Engineering

ISSN 2712-8172

journal homepage: http://engstroy.spbstu.ru/

DOI: 10.18720/MCE.98.7

Antiskid prediction model for cement pavements in seasonal frost regions

Q.Q. Zhao[a], H.T. Zhang*[b], R.S. Fediuk[c], J.W. Wang[d]

[a] Northeast Agricultural University, Harbin, Heilongjiang, China

[b] Northeast Forestry University, Harbin, Heilongjiang, China

[c] Far Eastern Federal University, Vladivostok, Russia

[d] Harbin Dongan Automobile Engine Manufacturing Co., Harbin, Heilongjiang, China

** E-mail: 2586762756@qq.com*

Keywords: concrete, pavement, numerical model, temperature, optimization

Abstract. The antiskid performance of the cement concrete pavement in the seasonal frost regions is an important factor determining the safety of road use. However, due to the low efficiency and high cost of on-site detection, it is very important to reasonably predict it. Five key factors such as ice film thickness, tire pressure, tire load, driving speed, and structural depth were determined. The response surface test was performed to determine the corresponding range of the five factors when the model was optimally predicted. A prediction model of antiskid performance for cement concrete pavement in the seasonal frost regions was created, the goodness of model fitting and the normal distribution of the model were tested, and the applicability of the model was verified. The results show that when the thickness of the ice film is 1.5 mm ～ 3 mm, the tire pressure is 180 kPa ～ 240 kPa, the driving speed is 40 km/h ～ 80 km/h, the structural depth is 0.24 mm ～ 0.62 mm and the tire load is 3250 N ～ 4000 N , the prediction level of the model is the best; SRI can be interpreted by the model accounting for 98.5 %, and the regression model has a high degree of fit, which meets the assumption of normal distribution; the model's SRI predicted value fits the field measured SRI value to 0.995, and the degree of fit is high. The prediction model of antiskid performance is of great significance to prolong the service life of cement concrete pavement in seasonal frost regions.

1. Introduction

The antiskid performances of the cement concrete pavement in the seasonal frost regions have a great influence on the performance of the pavement. The area of China's seasonal frost regions is 5.137 million square kilometers, accounting for 53.5 % of the total land area, and the area of seasonal frost regions and short-term frost regions in the world accounts for 25 % of the total land area. Therefore, the establishment of a scientific prediction model of the antiskid performance of the cement concrete pavement in the seasonal frost regions can reasonably predict the antiskid performance of the pavement, monitor the damaged state of the cement concrete pavement [1], carry out safety warning for the highway traffic, and extend the service life of the cement concrete pavement [2, 3], which is of great significance for timely pavement maintenance.

The research on antiskid performance prediction at internal and abroad mostly focuses on the qualitative analysis of antiskid performance factors, the review of evaluation methods of antiskid performance level and the influence of single factor antiskid performance [4−6]. It does not establish the relationship between antiskid performance and influencing factors, so it can not quantify the anti-slip performance. In a few models predicting antiskid performance, PIARC model [7] uses the relationship between speed constant and standard friction number to detect the antiskid performance in any speed range, but the influencing factors are single, which is not enough to comprehensively predict the sliding performance. Paper [8] integrated the statistical results of mixture gradation, aggregate structure and traffic level to establish the prediction model of antiskid performance. Usanava et al [9] established a model for estimation of polished stone value to study the influence of aggregate on antiskid performance, and ignored the change of anti-skid performance when the climate factor acts on the pavement aggregate. Dong Zheng [10] established a prediction model of long-term antiskid performance based on the optimized GA-BP neural network method, which has the limitation of

pavement service time and has a low prediction level for the overall antiskid performance of the pavement. Kane et al [11−14] according to the decomposition process of the pavement structure, it is confirmed that there is a certain relationship between the antiskid performance and the structure of the pavement, but the pavement structure can only be used as a part of the internal influence, and the research on the integrity of the antiskid performance is limited. Scientists [15, 16] established a model of antiskid performance and time, the model can stably predict the situation that the traffic volume tends to zero. Papers [17, 18] collected the accumulated traffic data of the road surface, established the soil volume reduction model, which can predict the antiskid performance of the road surface in different periods, but the prediction accuracy of the above models are low because the seasonal effect is not considered. Aliha et al [19] has carried out the braking test under different water film thickness, simulated the friction process of the tire rubber braking on the road, which has guiding significance for the tread pattern design that can improve the antiskid performance. The prediction model established by Xing et al [20] based on factors such as driving speed and water film thickness is more practical, but the influence of climate factors on antiskid performance is not considered. The antiskid performance of the cement concrete pavement in the seasonal frost regions is an important factor determining the safety of road use. However, due to the low efficiency and high cost of on-site detection, it is very important to reasonably predict it.

2. Methods

2.1. Screening of influencing factors for antiskid

In the selection of factors affecting the antiskid performance of cement concrete pavement, domestic and foreign experts have conducted relevant research. Dołżycki and Jaskuła [21] applied the heat machine friction model to study the effect of temperature on the friction between the tire and the road surface. It was found that the high temperature would reduce the hysteresis friction of the road surface and negatively correlated with the antiskid performance level of the road surface. Abirami et al [5] model tire and road confirmed that the contact stress between tire and road surface is large when tire load is too heavy and tire inflation pressure is insufficient, which has a positive impact on road antiskid. Guo et al [8] tested the antiskid of cement concrete specimen under different environmental conditions, and the results showed that the antiskid performance of the pavement is reduced under the environmental conditions such as water accumulation, oil stain, tire scrap and soil. Taryma [22] proposed tire type and tire pressure factors such as tread pattern and tread wear are important external factors affecting the antiskid performance of cement concrete pavement. Papers [23−32] has carried out the test of large vehicles acting on the road surface, evaluated the morphology change state of the aggregate on the road surface, and considered that the structural depth, material polishing degree and driving speed are the main factors controlling the antiskid performance. According to the investigation results of the actual traffic conditions of the road, Plati [33, 34] proposed that the pavement structure has a significant impact on the antiskid performance. Based on the research results of the above literature, the factors such as tire type, tire pressure, tread pattern, tread wear, structural depth, material polish, oil, soil and other road pollution, temperature, tire load, water film thickness and driving speed are obtained can affect the antiskid performance of cement concrete pavement.

In order to further verify whether the climatic factors can be used as important indicators to influence the antiskid performance, under the same environmental conditions that ensure the above-mentioned influencing factors, the antiskid performance of three sections with similar completion year, same investigation year, similar traffic flow, respectively in the seasonal frost regions, the short-term frost regions and the non-frost regions is tested, as shown in Fig. 1. The non-frost regions select the Longzhou Highway section of Guangdong Province, China, the short-term frost regions select the Kaiyang Expressway section of Jiangsu Province, China, and the seasonal frost regions selects the Zhaozhao Highway section of Heilongjiang Province, China. Each of the 3 sections has 15 piles, with the pile numbers ranging from K117 to K131. In Fig. 1, the horizontal coordinate is the pile number K117 ~ K131, the ordinate is the antiskid Index (SRI). According to China's standard for evaluation of highway technical conditions (JTGH20-2007), the calculation equation of SRI is as follows:

$$SRI = \frac{100 - SRI_{\min}}{1 + a_1 e^{a_2 SFC}} + SRI_{\min}, \quad (1)$$

where: SRI is the antiskid index; $SRI_{\min}$ is the limit value of antiskid performance, taken as 35; SFC is the lateral force coefficient; a_1 is the calibration coefficient, taken as 28.6; a_2 is the calibration coefficient, taken as − 0.105;

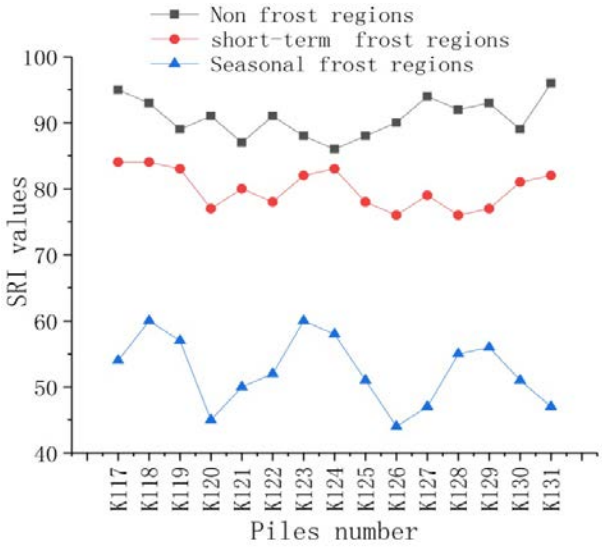

Figure 1. SRI values for different areas.

In Fig. 1, the SRI values corresponding to different stations in three different regions are different. For example, at K126, the SRI ratio of the non- frost regions to the seasonal frost regions is 2.09, and the ratio of the short-term frost regions to the seasonal frost regions is 1.79, which indicates that the SRI value of the seasonal frost regions is significantly lower than that of the short-term frost and the decrease of the SRI value in the short-term permafrost area is significantly higher than that in the non-frost regions. In Fig. 1, the SRI value of the non-frost regions is mostly between 90 and 100, and the antiskid performance is excellent. The SRI value of 15 stations in the short-term permafrost area varies from 75 to 90, the reason is that on the cement concrete pavement in the short-term frost soil area, the tire contacts with ice particles, water and road aggregate at the same time. The friction between the tire and the pavement is mainly composed of adhesion between the micro convex body of the friction pair surface and fluid shear. In this case, the SRI value of the pavement antiskid index is slightly lower than that of the non-frost soil pavement. Compared with the other two highways, the SRI value of the pavement in the seasonal frost regions is significantly lower, because the rain and snow on the cement concrete pavement in the seasonal frost regions will freeze to form ice film under the influence of the severe cold climate, and the pavement is covered by ice film, so that the friction between the pavement and the tire only depends on the interface adhesion and the deformation of the tire surface, and the SRI value is significantly lower than that in the short-term frost regions and non- frost regions. At the same time, there are usually 3 to 5 grades of northwest wind in the seasonal frost regions. Due to the wind force, the snow cover on the road is unevenly distributed and the thickness of the ice film is uneven, resulting in a significant difference in the SRI values of individual stations in the seasonal frost regions. For example, the SRI value of K120 is 21 % lower than that of K119.

In summary, the climatic factors have a significant impact on the antiskid performance of the pavement. In order to accurately predict the antiskid performance of cement concrete pavement in the seasonal frost regions, climate parameters that reflect the characteristics of the seasonal frost regions must be added to the prediction model. It is concluded from the above that the ice film thickness has a great influence on the antiskid performance index of the cement concrete pavement in the seasonal frost regions. Therefore, the ice film thickness factor is added to the antiskid performance prediction model for analysis. Combined with the previous research results, 12 influencing factors were extracted to screen the parameters of the model. Number 12 influencing factors, $F_1 - F_{12}$, as shown in Table 1.

Table 1. Influencing factors categories and numbers.

Number	Tire characteristic factors	Number	Road surface structure and medium factors	Number	Climate and traffic factors
F_1	Tire type	F_5	Structure depth	F_9	Temperature
F_2	Tire pressure	F_6	Material polishing degree	F_{10}	Driving speed
F_3	Tread pattern	F_7	Water film thickness	F_{11}	Tire load
F_4	Tread wear	F_8	Surface fouling, soil and other pollution	F_{12}	Ice film thickness

2.2. Identification of key factors

Based on the measured SRI data of Zhaozhao highway in Heilongjiang Province of China, the group analysis of the above 12 influencing factors is carried out, and the key factors influencing the model prediction

are screened out. The Euclidean distance method is used to calculate the group distance between the 12 factors. The factors with relatively small group distance are divided into the same group. Then the group distance between the groups is calculated by the Group Average Linkage method, and the two groups with the smallest group distance are rejoined into a group, and the number of the most reasonable groups determined by calculating the Silhouette index is 5, and the group distribution map is drawn by Statistical Package for Social Sciences (SPSS) software. The factors in the distribution map that affect the SRI value and the relatively large impact range can be identified as the key factors. The group classification and distribution are shown in Fig. 2.

In Fig. 2, the abscissa is the influence range standard value Z (RIV), and the ordinate is the influence degree standard value Z (SDV). The factors influencing the larger Z (RIV) and Z (SDV) values are the F_2 (tire pressure), F_5 (structural depth), F_{11} (tire load) in group 2, and F_{10} (driving speed) and F_{12} (ice film thickness) in group 3. It shows that the five factors in these two groups have a wide range of influence on antiskid performance, so these five factors are the main factors. The other three groups contain seven factors which are less influential than the five factors in group 2 and group 3, so they are secondary factors. After analyzing the grouping distribution results of 12 influencing factors, five factors including tire pressure, structural depth, driving speed, tire load and ice film thickness were identified as the key factors affecting the SRI value. They can be used as a parameter of the prediction model of the antiskid of the cement concrete pavement in the seasonal frost regions.

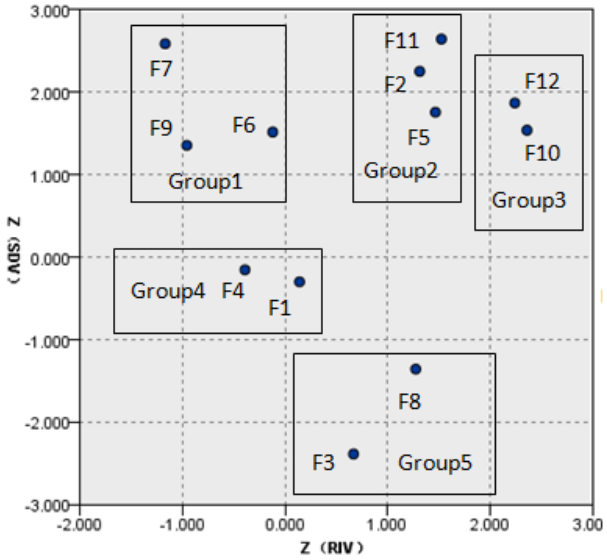

Figure 2. Grouping map.

2.3. Determination of model parameter value range

The antiskid performance prediction model of cement concrete pavement in the seasonal frost regions is constructed by using five parameters such as tire pressure, tire load, ice film thickness, driving speed and structural depth. It is necessary to determine the range of parameters. The parameters are denoted by symbols as follows: TP, TL, H, V and TD.

The range of 5 parameters should be reasonable and suitable for the characteristics of seasonal frost regions. If the TP value is too low or too high, the safety factor and driving comfort will be reduced. Therefore, the range of TP is selected within 180 kPa to 300 kPa. The TD range is obtained by calculating the ratio of groove depth and groove width multiplied by groove spacing. The groove width, groove depth and groove spacing commonly used in cement concrete pavement are 3−5 mm, 2−4 mm and 15−25 mm. The range of V is at highway speed 40 km/h ~ 120 km/h within the maximum and minimum limit value of degree. Too high TL value will cause damage to the road surface, so the common load value of 2500 ~ 4000 N is selected for TL range. According to the classification of road surface icing conditions studied by Smirnova et al [35], the ice film thickness is less than 1 mm when the ice layer is initially formed, and the driving condition is slightly slippery; the ice film thickness is 1 ~ 2 mm when partially frost, and the driving conditions are smooth; all frost When the ice film thickness is greater than 3 mm, the driving conditions are very smooth, and the road surface should not continue to drive, so the highest value of H does not exceed 3 mm.

2.4. Determination of the optimal prediction space of the model

According to the above five parameters, the response surface test is designed to determine the optimal prediction space for the antiskid performance prediction model of cement concrete pavement in the seasonal

frost zone. In order to facilitate the drawing of test records, the codes of TP, TL, H, V and TD in response surface test are A, B, C, D, and E. According to the number and range of parameters, five factors and three levels of response surface test were selected. The coding level and value are shown in Table 2.

Due to the positive relationship between SRI and friction coefficient in the research results of Highway Technical Status Assessment Standard (JTGH20-2007) and Smirnova [35], in order to simplify TP, TL, H, V and TD pairs SRI response surface drawing process, the ordinate of the response surface is set as the friction coefficient value, the abscissa is the factor value, and the degree of change of the friction coefficient value is the degree of change of the SRI value. Therefore, in the response surface analysis below, the change of ordinate value is still explained by the change of SRI value.

Table 2. 5 factor coding level and value.

Coding level	A(TP/kPa)	B(TL/N)	C(H/mm)	D(V/km/h)	E(TD/mm)
− 1	180	2500	1	40	0.24
0	240	3250	2	80	0.62
1	300	4000	3	120	1

In the case where the coding levels of T, V, and TD are 0, the response surface of the design H (mm) and TP (kPa) to the SRI value is as shown in Fig. 3(a). When H was between 1 mm and 1.5 mm, the SRI value increased slightly, because the initial ice sheet was crushed and the edges of the crushed ice were convex and the cutting and furrow functions between the sharp corners and the tires increased the SRI value while increasing the lagging resistance; when H is increased from 1.5 mm to 3 mm, the inclination of the response surface is significantly increased from 1 mm to 1.5 mm. The reason is that the 3 mm ice film is compact and flat. Under the action of vehicle driving friction, the completely frost ice film surface will produce only a few molecular thick water films and enter into the boundary lubrication state. The adhesion friction between tire and ice surface drops sharply, and the SRI value drops the most. At this time, the SRI is the most sensitive to the change of H and has the highest response. Observe the surface change of TP in Fig. 3(a). As the TP increases, the contact area between the tire and the road surface decreases, and the SRI value decreases. When the TP is 180 kPa to 240 kPa, the slope of the surface is larger than that of 240 kPa to 300 kPa, and the SRI value is significantly reduced. The reason is that the deformation of the tire is the most serious in this interval and the contact area with the road surface changes most obviously, therefore, in the range of 180 KPa to 240 kPa, SRI has the highest response to TP.

In the case where the coding levels of TP, V, and H are 0, the response surface of the design TL (N) and TD (mm) to the SRI value is as shown in Fig. 3(b). After the TD exceeds 0.62 mm, the response surface gradually flattens. The reason is that when the structural depth of the groove reaches 0.62 mm, although reducing the slot spacing, increasing the slot depth or increasing the slot width can increase the TD value, the SRI value will not increase with it. At this time, the response of SRI to TD change is the lowest. Observe the surface change of TL in Fig. 3(b). When the TL exceeds 3250 N and close to 4000 N, the slope of the response surface increases obviously compared with 2500 N to 3250 N. The reason is that the road surface is pressed into the tire with heavy load, and the contact area between the tire and the road surface is from the tire. The center area is turned to the sides of the tire, and the grounding compressive stress becomes significantly larger as the tire sinks, so that the SRI value is significantly increased compared with the light load, indicating that the SRI has a higher responsiveness to the TL range above 3250 N.

In the case where the TL, TP, and H coding levels are zero, the response surface of the design V (km/h) and TD (mm) to the SRI value is as shown in Fig. 3(c). When V gradually increases from 80 km/h to 120 km/h, the inclination of the response surface is less than 40 km/h to 80 km/h, because the tire can be in full contact with the macroscopic structure of the road surface at low speed, and the higher the V, the smaller the actual contact area, the actual contact area between the tire and the road surface is gradually constant after the V exceeds 80 km/h, so the variation of the SRI value tends to be flat, indicating that the SRI has a lower response to V when the V range is above 80 km/h.

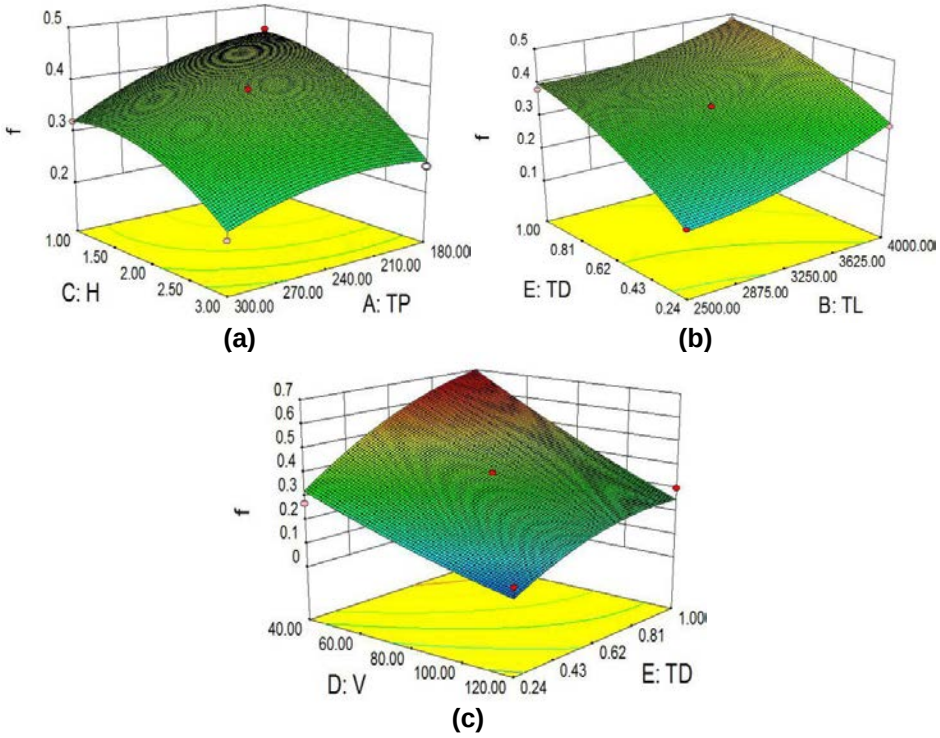

Figure 3. Response surface of five parameters to SRI: (a) TP and H response surface to SRI values (b) TL and TD response surface to SRI values (c) V and TD response surface to SRI values.

Combined with the above analysis of the response surface, if the response surface approaches the gradual, it means that the SRI value cannot change synchronously with the parameter value within the range of parameters corresponding to the surface, and the SRI responds to the change of parameters is low, at this time, the prediction accuracy of the antiskid performance prediction model of cement concrete pavement is low. If the slope of the response surface is large, the SRI value changes significantly, and the corresponding parameter range is more suitable for model prediction. According to the results of response surface analysis, the parameters of H value is 1.5 mm ~ 3 mm, TP value is 180 kPa ～ 240 kPa, TL value is 3250 N ～ 4000 N, TD value is 0.24 mm ～ 0.62 mm, V value is 40 km/h ～ 80 km/h, the range of values is the optimal prediction space of the model. When the five parameters are in the optimal prediction space, the prediction level of the model is the best.

3. Results and Discussion

3.1. Establishment of Model Relationship

By analyzing the variance of the response surface test results, the primary and secondary influence degree values of each parameter on the SRI value can be obtained, thereby integrating the parameters and establishing the relationship between the SRI and the parameters. After removing the source of variation with a small F value, the results of the variance analysis of 5 parameters were retained, and are shown in Table 3.

Table 3. Variance analysis of parameters.

Source	Sum of Squares	df	Mean Square	F	P
Model	0.35	5	0.07	52.994	< 0.001
TP	0.005	1	0.005	8.287	0.026
TL	0.007	1	0.007	13.750	0.009
H	0.036	1	0.036	66.065	< 0.001
V	0.034	1	0.034	43.750	< 0.001
TD	0.021	1	0.021	39.676	< 0.001
Residual	0.003	19	0.000	–	–
Lack of fit	0.001	14	0.000	0.368	0.9573
Pure Error	0.001	5	0.000	–	–
Total	0.353	24	–	–	–

In Table 3, the ratio of the squared sum of the regressions of the factors to the degrees of freedom (the mean square) is much higher than the mean square of the residuals, and the pure error term is close to 0, indicating that the experimental error is small. The significance value p of each factor is less than 0.05; the p value of the lack of fit is 0.9573, which is close to 1, indicating that the five parameters have a significant effect on the SRI. The higher the F value, the greater the degree of influence, the F value of ice film thickness is 66.065, which is the largest F value compared with the other four parameters. The F value of driving speed and structural depth is relatively close and the size is middle, respectively 43.750 and 39.676. The F values of tire load and tire pressure are similar to the other three parameters, which are 13.750 and 8.287, respectively. After the above analysis, the effect of ice film thickness on SRI value is most significant, followed by driving speed and structural depth, and finally tire load and tire pressure. Therefore, when establishing the relationship between parameters and SRI, the ice film thickness is listed as a separate indicator, and the driving speed and structural depth, tire load and tire pressure are respectively integrated into a comprehensive index. With reference to the prediction model of antiskid performance in the form of exponential function established by parameters such as water film thickness of Xing [20], the relationship between SRI and ice film thickness, tire pressure, tire load, driving speed and structural depth is established as follows:

$$SRI = \lambda \cdot (TP/TL)^{\lambda_1} \cdot H^{\lambda_2} \cdot \exp \lambda_3 \cdot \left[(60-V)/TD\right] \tag{2}$$

where SRI is the antiskid index; TP is the tire inflation pressure (kPa); TL is the load applied to the tire (N); H is the ice film thickness on the road surface (mm); V is between the road surface and the tire Relative slip speed (km/h); TD is the pavement structure depth (mm); λ, λ_1, λ_2 and λ_3 are regression coefficients.

Since equation (2) is a nonlinear equation, in order to simplify the method and steps of nonlinear equations in regression analysis, a logarithmic function method is used to linearly transform the equation. To find the natural logarithm of both sides of the equation, the equation turned into:

$$\ln SRI = \ln \lambda + \lambda_1 \ln(TP/TL) + \lambda_2 \ln H + \lambda_3 (60-V)/TD \tag{3}$$

Let $\ln SRI = y$, $\ln \lambda = \lambda_0$, $\ln\left(TP/TL\right) = x_1$, $\ln H = x_2$, $\left(60-V\right)/TD = x_3$.

Then equation (3) can be converted into:

$$y = \lambda_0 + \lambda_1 x_1 + \lambda_2 x_2 + \lambda_3 x_3 \tag{4}$$

The original nonlinear equation can be transformed into a linear equation for solving.

3.2. Significance test of regression equation

From the typical section of the seasonal frost regions, the field survey data of 20 sections of the three roads of Zhaozhao Highway, Heda Expressway and Hazhao Highway are selected for regression analysis. According to equation (4), the SRI value of the on-site survey is set to correspond to the transformation y as the dependent variable, TP and TL correspond to the transformed x_1, H corresponding transformed x_2, V and TD corresponding transformed x_3 as independent variables, and the model is linearly tested. In Table 4, the regression sum of the dependent variables is 60.544, and the ratio of the squared regression to the mean square is 20.181, which is much higher than the mean square of the residual 0.071. The ratio of the mean regression squared to the sum of the squared mean residuals (F) is 274.339, the value is large, and indicating that the change of the dependent variable is caused by the change of the independent variable rather than the experimental error, and the independent variable has a high explanatory force for the dependent variable. The significance value is 0, less than 0.05, the model linear regression significant. It is shown that in the F test, the linear regression of the equation is obvious, and a linear model can be established between the dependent variable and the independent variable.

Table 4. Regression model of ANOVAs.

model		Sum of Squares	df	Mean Square	F	Sig.
1	Regression	60.544	3	20.181	274.339	0
	Residual	0.786	11	0.071	–	–
	Total	61.330	14	–	–	–

3.3. Significance test of regression coefficient

After the F test shows that the linear model can be established, it is necessary to determine whether the influence of the independent variable on the dependent variable is significant. Therefore, the regression coefficient should be tested for significance. In Table 5, the partial regression coefficient represents the weight of each index. The absolute value of the standardized partial regression coefficient indicates the degree of influence of each variable on the dependent variable. The absolute value of the standardized partial regression coefficient of x_2 is the largest among the three indicators, indicating the parameter H corresponding to x_2 has

the greatest influence on SRI value, the x_3 corresponding parameter V and TD influence degree is second, and the relatively small degree of influence is the x_1 corresponding parameter TP and TL. This is consistent with the analysis of variance when determining the relationship between parameters and SRI. The standard error of the partial regression coefficient of each parameter is small, the Sig. significance value is less than 0.05, and the absolute value of the bilateral test threshold t is all greater than the significance level, indicating that the independent variable has significant influence, and the independent variable is retained in the model.

Table 5. Coefficient of regression model.

Parameter	Partial regression coefficient	Partial regression coefficient standard error	Standardized partial regression coefficient	t	Sig.
Constant	2.808	0.216	-	15.048	0.003
x_1	-0.513	0.041	-0.224	-6.575	0.012
x_2	-0.199	0.117	-0.811	-24.328	0.005
x_3	0.005	0.001	0.652	17.338	0.009

Bring the results of the above regression analysis into equation (4), the model is expressed as:

$$y = 2.808 - 0.513x_1 - 0.199x_2 + 0.005x_3 \tag{5}$$

Reconverted to a nonlinear equation:

$$SRI = 16.58\left(TP/TL\right)^{-0.513} H^{-0.199} \exp\left[0.005\left(60 - V\right)/TD\right] \tag{6}$$

where SRI is the antiskid index; TP is the tire inflation pressure (kPa); TL is the load applied to the tire (N); H is the ice film thickness on the road surface (mm), $H \leqslant 3$ mm； V is between the road surface and the tire Relative slip speed (km/h); TD is the pavement structure depth (mm).

3.4. Model goodness of fit test

After the antiskid performance prediction model of cement concrete pavement in the seasonal frost regions is established, the goodness of fit between the independent variable and the dependent variable should be tested to ensure that the dependent variable can be interpreted by the model. In Table 6, R^2 is the deterministic coefficient between the dependent variable and the independent variable. Adjusting R^2 is the mean square error ratio that eliminates the influence of the number of independent variables. The closer R^2 and the adjusted R^2 are to 1, the better the fitting effect of the regression equation. The regression equation has an adjustment of R^2 of 0.985, which is close to 1, and the standard estimation error is only 0.113, indicating that the model has a good goodness of fit, and the dependent variable can be accounted for 98.5 % by the model interpretation.

Table 6. Summary of regression models.

R^2	Adjust R^2	Standard estimated error
0.992	0.985	0.113

3.5. Model normal distribution test

In order to verify the applicability of the prediction model of the antiskid performance of the cement concrete pavement in the seasonal frost regions, the normal distribution test was carried out for the model. Observing the residual histogram and the normal distribution curve of Fig. 4, the sample size is large enough and the residual distribution conforms to the normal distribution, which proves the correctness of the prediction model. Observe the residual P-P graph of Fig. 5, the residual distribution curve changes around the pre-set diagonal and diagonal directions. The two are close to coincide, and the regression model satisfies the normal distribution hypothesis. In summary, the SRI prediction model established by using TP, TL, H, V and TD as parameters has passed various tests, and the regression effect is remarkable, and the goodness of fitting is high.

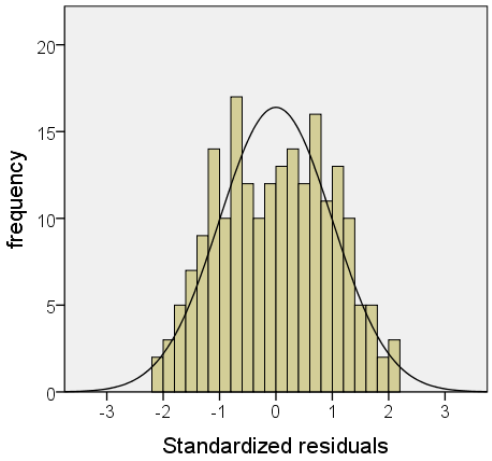

Figure 4. Residual histogram.

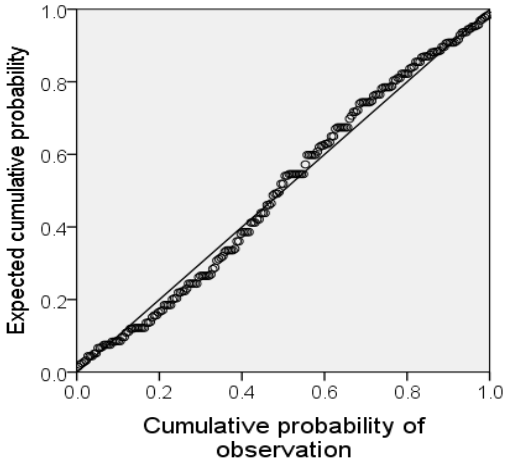

Figure 5. Residual regression P-P diagram.

3.6. Model verification

In order to verify the practicability of the antiskid performance prediction model of cement concrete pavement in the seasonal frost regions, the measured value of SRI and the predicted value of the model in a section of Zhaozhao highway in the past 9 years are selected for verification. The predicted value of SRI of the prediction model and PIARC model [7] are respectively matched with the measured value of SRI by SPSS software. In Fig. 6, the abscissa is the SRI measured value km, the ordinate is the SRI predicted value kp, the deterministic coefficient R^2 of the PIARC model SRI predicted value and the measured value is 0.852, and the deterministic coefficient R^2 of the predicted model SRI predicted value and the measured value is fitted, it is 0.995, which proves that the prediction model has a higher degree of fit.

The test points for model verification on a highway section may lack randomness and result in deviation of results. Therefore, the measured SRI data of the six roads of the three roads of Zhaozhao Highway, Heda Expressway and Hazhao Highway are verified again in the same year. As shown in Fig. 7, the abscissa is the numerical number of 6 road segments in turn, and the ordinate is the SRI value, and the SRI value curve under different road segments is drawn. Since the ice film thickness of each of the six sections is not completely the same, according to the above response surface analysis results, when the ice film thickness of the road section is in the best prediction space of 1.5 mm to 3 mm, the SRI prediction value of the model will be close to or lower than the actual measurement Value, the SRI prediction value in other prediction space will be higher than the measured value, so the SRI prediction value of different road sections has higher or lower difference than the measured value. At the same time, it can be observed that the predicted model SRI predictive value curve is closer to the SRI measured value curve than the PIARC model SRI predicted value curve, which proves that the predictive model predicts the SRI value better, and the predictive model has good practicability.

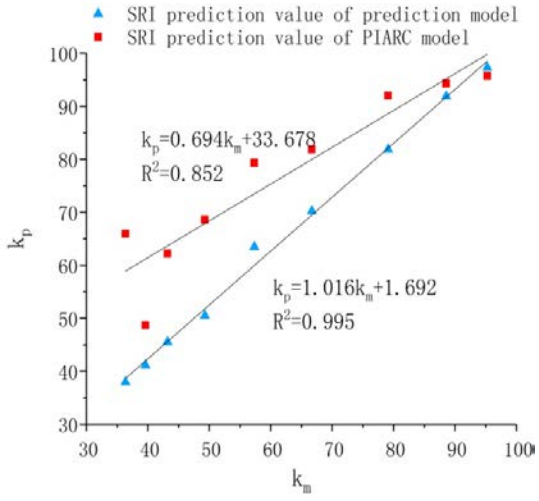

Figure 6. SRI predicts the correlation between the measured value and the measured value.

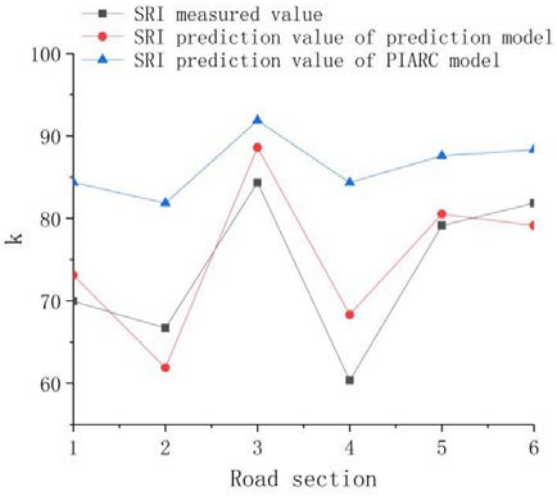

Figure 7. SRI prediction effect of prediction model.

4. Conclusions

1. The climatic factors have a significant impact on the antiskid performance of cement concrete pavement. The key factors affecting the antiskid performance of cement concrete pavement in the seasonal frost regions are ice film thickness, tire pressure, tire load, driving speed and structural depth. The test statistic value (F) of each factor is larger, which means that the influence degree of factor on antiskid performance is higher. The F value of the ice film thickness is 66.065, the F value of the driving speed is 43.750, the F value of the construction depth is 39.676, the F value of the tire load is 13.750, and the F value of the tire pressure is 8.287. It shows that the effect of ice film thickness on SRI value is most significant, followed by driving speed and construction depth, and finally tire load and tire pressure.

2. When the ice film thickness ranges from 1.5 mm to 3 mm, the tire pressure is between 180 kPa and 240 kPa, the driving speed is between 40 km/h and 80 km/h, the structural depth is between 0.24 mm and 0.62 mm, and the tire load is between 3250 N and 4000 N, the SRI's responsiveness to parameter changes is higher than other parameter values, which is the optimal prediction space of the model. At this time, the model's prediction level is optimal.

3. Using the five parameters of ice film thickness, tire pressure, tire load, driving speed and structural depth, the SRI value of the antiskid performance index of the cement concrete pavement in the seasonal frost regions can be predicted, and the ice film thickness in the prediction model is a separate indicator. Tire pressure and tire load, driving speed and structural depth are combined into a comprehensive index. The function forms of the index are exponential functions, and the coefficients after regression are -0.513, -0.199 and 0.005. The predictive model has a decisive coefficient R^2 of 0.985 and a significance level of 0. The model has a high degree of fit and significant regression, indicating that the predictive model has statistical applicability.

4. The prediction model and the PIARC model are verified in the same period of different sections and different sections of the same section. The R^2 of the prediction model is 0.995, the R^2 of the PIARC model is 0.852, and compared with the PIARC model, the SRI value predicted by the prediction model is closer to the measured value of SRI. It indicates that the prediction model of the antiskid performance of cement concrete pavement in the seasonal frost regions has a high prediction level and is highly practical.

5. Acknowledgements

Project Support: Youth Talent Project of Northeast Agricultural University (54978412).

References

1. Gao, J., Wang, H., Chen, J., Meng, X., You, Z. Laboratory evaluation on comprehensive performance of polyurethane rubber particle mixture. Construction and Building Materials. 2019. 224. Pp. 29–39.
2. Ueckermann, A., Wang, D., Oeser, M., Steinauer, B. A contribution to non-contact skid resistance measurement. International Journal of Pavement Engineering. 2015. 16(7). Pp. 646–659.
3. Zhao, Q., Cheng, P., Wang, J., Wei, Y. Damage prediction model for concrete pavements in seasonal frost regions. Magazine of Civil Engineering. 2018. 84(8). Pp. 57–66. doi: 10.18720/MCE.84.6.
4. De Larrard, F., Martinez-Castillo, R., Sedran, T., Hauza, P., Poirier, J.E. Cementitious artificial aggregate particles for high-skid resistance pavements. Road Materials and Pavement Design. 2012. 13(2). Pp. 376–384.
5. Abirami, T., Loganaganandan, M., Murali G., Fediuk, R., Vickhram Sreekrishna, R., Vignesh, T., Januppriya, G., Karthikeyan K. Experimental research on impact response of novel steel fibrous concretes under falling mass impact. Construction and Building Materials. 2019. 222. Pp. 447–457.
6. Klyuev, S.V., Klyuev, A.V., Vatin, N.I. Fiber concrete for the construction industry. Magazine of Civil Engineering. 2018. 84(8). Pp. 41–47. doi: 10.18720/MCE.84.4.
7. Denisova, Yu.V. Additive technology in construction. Construction Materials and Products. 2018. 1(3). Pp. 33 – 42.
8. Guo, R., Nian, T., Li, P., Fu, J., Guo, H. Anti-erosion performance of asphalt pavement with a sub-base of cement-treated mixtures Construction and Building Materials. 2019. 223. Pp. 278−287.
9. Usanova, K., Rybakov, V., Udalova, V., Kovylkov, A. Examination of Quality and Operational Properties of Vibropressed Paving Elements. MATEC Web of Conferences. 2016. 73. 040131.
10. Zheng, D., Qian, Z., Liu, Y., Liu, C. Prediction and sensitivity analysis of long-term skid resistance of epoxy asphalt mixture based on GA-BP neural network. Construction and Building Materials. 2018. 158. Pp. 614−623. https://doi.org/10.1016/j.conbuildmat.2017.10.056.
11. Kane, M., Rado, Z., Timmons, A. Exploring the texture-friction relationship: From texture empirical decomposition to pavement friction. International Journal of Pavement Engineering. 2015. 16(10). Pp. 919–928.
12. Lin, C., Tongjing, W. Effect of fine aggregate angularity on skid-resistance of asphalt pavement using accelerated pavement testing. Construction and Building Materials. 2018. 168. Pp. 41−46. URL: https://doi.org/10.1016/j.conbuildmat.2018.01.171.
13. Fediuk, R., Smoliakov, A., Muraviov, A. Mechanical Properties of Fiber-Reinforced Concrete Using Composite Binders. Advances in Materials Science and Engineering. 2017. Pp.1-13. https://doi.org/10.1155/2017/2316347
14. Klyuev, S.V., Klyuev, A.V., Vatin, N.I. Fine-grained concrete with combined reinforcement by different types of fibers. MATEC Web of Conferences. 2018. No. 245, 03006.
15. Fediuk, R.S., Lesovik, V.S., Liseitsev, Yu.L., Timokhin, R.A., Bituyev, A.V., Zaiakhanov, M.Ye., Mochalov, A.V. Composite binders for concretes with improved shock resistance. Magazine of Civil Engineering. 2019. 85(1). Pp. 28–38. DOI: 10.18720/MCE.85.3.

16. Nelyubova, V.V., Babayev, V.B., Alfimova, N.I., Usikov, S.A., Masanin, O.O. Improving the efficiency of fibre concrete production. Construction Materials and Products. 2019. 2 (2). Pp. 4-9.
17. Yong-hong, Y., Yuan-hao, J., Xuan-cang, W. Pavement Performance Prediction Methods and Maintenance Cost Based on the Structure Load. Procedia Engineering. 2016. 137. Pp. 41−48.
18. Horníček, L., Rakowski, Z. Mechanical Stabilization of Intermediate Granular Layers in Pavement Structures – Laboratory Study Procedia Engineering. 2017. 189. Pp. 174−180.
19. Aliha, M.R.M., Bahmani, A., Akhondi. Sh. A novel test specimen for investigating the mixed mode I+III fracture toughness of hot mix asphalt composites – Experimental and theoretical study. International Journal of Solids and Structures. 2016. 90, Pp. 167−177.
20. Xing, B., Fan, W., Zhuang, C., Qian, C., Lv, X. Effects of the morphological characteristics of mineral powder fillers on the rheological properties of asphalt mastics at high and medium temperatures. Powder Technology. 2019. 348. Pp. 33−42.
21. Dołżycki, B., Jaskuła, P. Review and evaluation of cold recycling with bitumen emulsion and cement for rehabilitation of old pavements. Journal of Traffic and Transportation Engineering (English Edition). 2019. 6(4). Pp. 311−323.
22. Taryma, T., Ejsmont, J.A., Ronowski, G., Swieczko-Zurek, B., Mioduszewski, P., Drywa, M., Woźniak, R. Road Texture Influence on Tire Rolling Resistance. Key Engineering Materials. 2013. 597. Pp. 193−198.
23. Guan, B., Wu, J., Xie, C., Fang, J., Zheng, H., Chen, H. Influence of macrotexture and microtexture on the skid resistance of aggregates. Advances in Materials Science and Engineering. 2018. Pp. 1–9.
24. Mengue, E., Mroueh, H., Lancelot,L, Medjo Eko, R. Design and parametric study of a pavement foundation layer made of cement-treated fine-grained lateritic soil. Soils and Foundations, 2018. 58(3). Pp. 666−677.
25. Shi, X., Mukhopadhyay, A., Zollinger, D. Sustainability assessment for portland cement concrete pavement containing reclaimed asphalt pavement aggregates. Journal of Cleaner Production. 2018. 192. Pp. 569−581.
26. Rezaei, A., Masad, E. Experimental-based model for predicting the skid resistance of asphalt pavements. International Journal of Pavement Engineering. 2013. 14(1). Pp. 24–35.
27. Farhan, A.H., Dawson, A.R., Thom, N.H., Adam, S., Smith, M.J. Flexural characteristics of rubberized cement-stabilized crushed aggregate for pavement structure. Materials & Design. 2015. 88. Pp. 897−905.
28. Qian, Z., Meng, L. Study on micro-texture and skid resistance of aggregate during polishing. Frontiers of Structural and Civil Engineering. 2017. 11(3). Pp. 346–352.
29. Huang, B., Shu, X., Li, G. Laboratory investigation of portland cement concrete containing recycled asphalt pavements. Cement and Concrete Research. 2005. 35(10). Pp. 2008−2013.
30. Chindaprasirt, P., Sujumnongtokul, P., Posi, P. Durability and Mechanical Properties of Pavement Concrete Containing Bagasse Ash. Materials Today: Proceedings. 2019. 17(4). Pp. 1612−1626.
31. Alenezi, T., Norambuena-Contreras, J., Dawson, A., Garcia, A. A novel type cold mix pavement material made with calcium-alginate and aggregates. Journal of Cleaner Production. 2019. 212. Pp. 37−45.
32. Gupta,T., Sachdeva, S.N. Laboratory investigation and modeling of concrete pavements containing AOD steel slag. Cement and Concrete Research. 2019. 124. 105808.
33. Plati, C., Pomoni, M. Impact of Traffic Volume on Pavement Macrotexture and Skid Resistance Long-Term Performance. Transportation Research Record. 2019. 2673(2). Pp. 314–322.
34. Plati, C., Pomoni, M., Stergiou, T. Development of a mean profile depth to mean texture depth shift factor for asphalt pavements. Transportation Research Record. 2017. 2641(1). Pp. 156–163.
35. Smirnova, O., Kharitonov, A., Belentsov, Y. Influence of polyolefin fibers on the strength and deformability properties of road pavement concrete. Journal of Traffic and Transportation Engineering (English Edition). 2019. 6(4). Pp. 407-417.

Contacts:

Qianqian Zhao, 492954791@qq.com
Hetong Zhang, 2586762756@qq.com
Roman Fediuk, roman44@yandex.ru
Jianwu Wang, nihaone@163.com